A Study on REMPI as a Measurement Technique for Highly Rarefied Gas Flows*
(Analyses of Experimental REMPI Spectra in Supersonic Free Molecular Flows)

Hideo MORI**, Toshihiko ISHIDA**,
Yoshinori AOKI** and Tomohide NIIMI**

A technique for measurement of thermodynamic variables with high sensitivity is necessary for analyses of highly rarefied gas flows, gas-surface interaction, and so on. REMPI (Resonantly Enhanced Multiphoton Ionization) is a powerful optical tool because of its high sensitivity even in highly rarefied gas flows and its ability to measure nonequilibrium amongst internal (translational, vibrational, and rotational) energy modes. In this paper, a REMPI system is developed and REMPI spectra are measured on the center line of a free-molecular flow. The fundamental properties of the REMPI signal are also described. A method using a Boltzmann plot with the spectral lines of multiple branches is proposed, and the ratio of the electronic transition dipole moments in the two-photon Hönl-London factors for the O and P branches is determined.

Key Words: Rarefied Gas, Flow Measurements, Laser-aided Diagnostics, REMPI, Nitrogen, Boltzmann Plot

1. Introduction

In recent years, analyses of highly rarefied gas flows and behaviors of gas molecules interacting with solid surfaces have been very important for development of vacuum science and aerospace engineering, generating strong demand for measurement methods for highly rarefied gas flows. Spectroscopic methods, which are non-intrusive and species-selective, have been used for the measurement of thermodynamic variables in gaseous flows and have also enabled the analysis of nonequilibrium in rarefied gas flows. Thus far, several spectroscopic methods such as Electron Beam Fluorescence (EBF)[1], Laser Induced Fluorescence (LIF)[2] and Coherent Anti-Stokes Raman Scattering (CARS)[3] have been developed, and each method is applied to diagnoses of gaseous flows in a range of number density appropriate for the method. However, since these techniques are based on the detection of fluorescence or scattered light, even LIF, which is the most sensitive method among them, can hardly be applied to the rarefied gas flow below 10^{12} molecules/cm^3 [1].

The resonantly enhanced multiphoton ionization (REMPI) was selected to measure rotational temperatures in highly rarefied gas flows. REMPI is a technique for ionization of molecules by multiphoton absorption. Unlike nonresonant multiphoton ionization, molecules are ionized via the resonant state, leading to very high ionization probability. Because REMPI has a very high sensitivity, it can be applied to the measurement of aerodynamic variables, such as temperature and number density, in highly rarefied gas flows below the number density of 10^{12} molecules/cm^3, which is too low to detect by conventional methods such as LIF. For N_2-REMPI, the sensitivities of 10^9 molecules/cm^3 for 2R+2 REMPI[4] and 10^5 molecules/cm^3 for 2R+1 REMPI[5] have been reported.

* Received 14th March, 2001. Japanese original: Trans. Jpn. Soc. Mech. Eng., Vol. 66, No. 645, B (2000), pp. 1373-1379 (Received 15th July, 1999)

** Department of Electronic-Mechanical Engineering, Nagoya University, Furo-cho, Chikusa-ku, Nagoya 464-8603, Japan. E-mail: mori@suelab.nuem.nagoya-u.ac.jp

In a previous paper[6], the fundamental properties of 2R+2 N_2-REMPI spectra, such as temperature dependence and the spectral lines appropriate for the Boltzmann plot, were clarified by spectral simulations. However, since for the conventional Boltzmann plot we cannot use spectral lines of multiple branches, the number of the spectral lines is limited for the plot, leading to the inaccuracy of the deduced rotational temperature. This problem arises from the great difficulty in determining the electronic transition factors of the two-photon Hönl-London factors theoretically.

An experimental apparatus for the measurement of rotational temperature of nitrogen by 2R+2 REMPI has been developed. Using this apparatus, the REMPI spectra on the center line of free-molecular jets are measured, and the rotational temperature is deduced from the slope of the Boltzmann plot as mentioned in the previous paper[6]. Then we investigate the dependence of the REMPI signal intensity on the laser flux and the number density for our apparatus. Moreover, we propose the new method of the Boltzmann plot using the spectral lines of both O and P branches by determining the ratio of the electronic transition factors of these branches experimentally. This ratio also introduces the possibility of fitting the theoretical spectra to the experimental data, to obtain rotational temperature measurements.

2. 2R+2 N_2-REMPI Spectra

Figure 1 depicts the modeling of 2R+2 N_2-REMPI. In this process, nitrogen molecules at the ground state ($X^1\Sigma_g^+$) are excited to the resonant state ($a^1\Pi_g$) by two-photon absorption. Then the excited molecules are ionized by additional two-photon energy. Because four photons participate in this process, the ion current is proportional to the fourth power of laser flux when the flux is relatively low. On the other hand, when the laser flux is sufficiently high so that almost all the excited molecules ionize, the ion current is proportional to the second power of laser flux, because the REMPI process reflects the two-photon transition process from the ground state to the resonant one[6]. In this case, since the REMPI spectra depend on the rotational energy distribution at the ground state, the rotational energy distribution, i.e., the rotational temperature, can be deduced from the REMPI spectra.

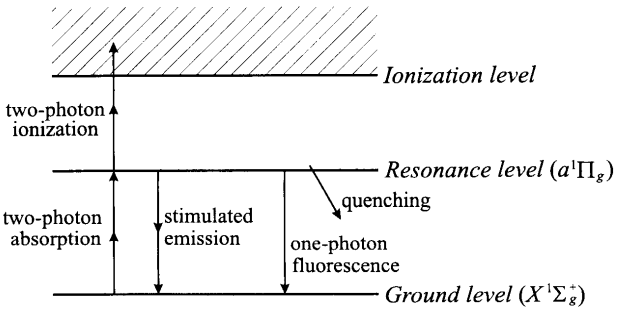

Fig. 1 Modeling of 2R+2 N_2-REMPI

When the laser flux is constant, the rotational line intensity $I_{J',J''}$ in 2R+2 N_2-REMPI spectra is given by[4),(7)]

$$I_{J',J''}=Cg(J'')S(J',J'')\exp(-E_{rot}/kT_{rot}) \quad (1)$$

where C is the constant independent of the rotational quantum number J' of the resonant state and J'' of the ground state, but including Franck-Condon factor, laser flux, number density of the molecules, and so on. $g(J'')$ is the nuclear spin degeneracy of nitrogen molecules formed by N^{14} atoms, whose value is 3 and 6 for odd and even J'', respectively. E_{rot} is the rotational energy, k the Boltzmann's constant, and T_{rot} the rotational temperature.

$S(J',J'')$ is the two-photon Hönl-London factor for the $a^1\Pi_g \leftarrow X^1\Sigma_g^+$ transition. In Table 1, the values of $S(J',J'')$ for linearly polarized light[7)-9)] are listed (in this table, $\Delta J=J'-J''$). The $M(O)$-$M(S)$ in Table 1 are the transition factors given by the products of the electronic transition dipole moments. These factors depend not on J'' but on the kind of the branches. Generally, it is impossible to determine the factors theoretically because the electronic transition dipole moments for the transitions via virtual states are unknown[9].

Since the signal intensity $I_{J',J''}$ is related to the rotational energy E_{rot}/k as described in Eq.(1), rotational temperatures can be easily deduced from the measured REMPI spectra by the Boltzmann plot. As mentioned above, spectral lines of one branch have been used for the conventional Boltzmann plot, because the $M(O)$-$M(S)$ in the two-photon Hönl-London factors, which depend on the kind of the branch, are unknown. However, a Boltzmann plot using spectral lines belonging to multiple branches is possible if M's can be determined from the experimental REMPI spectra. This increases the number of

Table 1 Two-photon Hönl-London factors of nitrogen for the $a^1\Pi_g \leftarrow X^1\Sigma_g^+$ transition using linearly polarized light

Branch		$S(J'')$
O	($\Delta J=-2$)	$M(O)J''(J''-2)/15(2J''-1)$
P	($\Delta J=-1$)	$M(P)(J''+1)/30$
Q	($\Delta J=0$)	$M(Q)(2J''+1)/10(2J''-1)(2J''+3)$
R	($\Delta J=1$)	$M(R)J/30$
S	($\Delta J=2$)	$M(S)(J''+1)(J''+3)/15(2J''+3)$

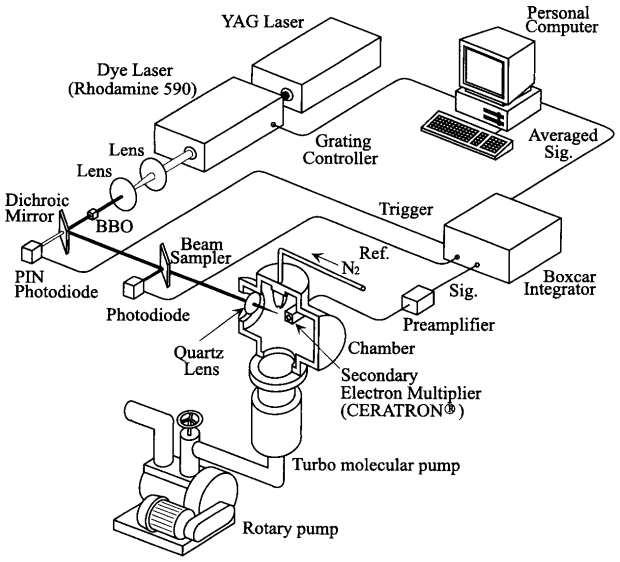

Fig. 2 Experimental apparatus

spectral lines available for the Boltzmann plot and leads to a more accurate temperature.

3. Experimental Apparatus

Figure 2 shows the experimental apparatus. The vacuum chamber is evacuated by two turbo molecular pumps in parallel. Nitrogen gas is issued via a sonic nozzle, whose diameter D is 0.50 mm, into the chamber. For the stagnation pressure of 0.60 Torr (80 Pa) and the temperature of 294 K, the background pressure in the chamber is kept at 3.3×10^{-5} Torr (4.4×10^{-3} Pa).

A Nd-YAG pumped dye laser (Spectra-Physics, DCR-3D(10) and PDL-2) with Rhodamine 6 G dye is used as the laser source, and the output is frequency-doubled by a BBO crystal. The wavelength of the laser beam is near 283.6 nm. The beam is focused through a quartz lens ($f=120$ mm) on the center line of the nitrogen free-molecular flow. The beam diameter at the focal point is 1.0×10^{-4} m. The energy, repetition rate, and duration time of the laser beam are 11.3 mJ/pulse, 10 Hz, and 7 ns, respectively. In this case, the average laser flux at the focal point is 2.94×10^{32} photons/m^2·sec at the wavelength of 283.6 nm.

The ionized nitrogen molecules are detected by a secondary electron multiplier (Murata, CERATRON® EME-2061C). To collect the ions by the detector effectively, an anode plate (repeller) and two cathode plates with a hole ($\phi=10$ mm, the same diameter as the entrance of the detector), which act as "lenses" for electric field, are mounted in front of the detector as shown in Fig. 3. The voltages applied to the electrodes were adjusted so that the ion signal was detected most efficiently. As a result, the voltages applied to

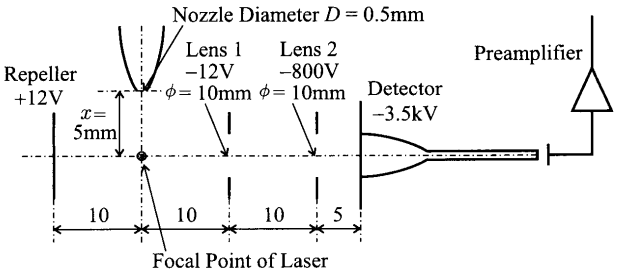

Fig. 3 Detection system

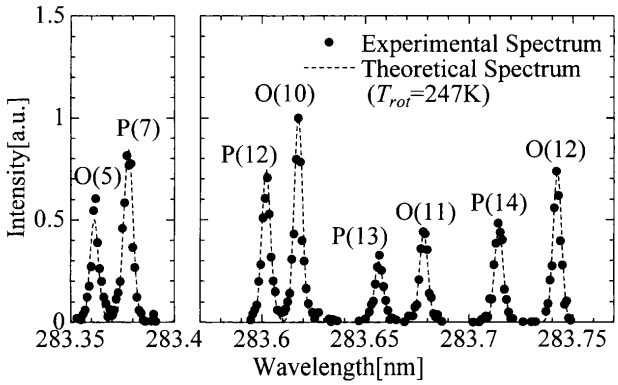

Fig. 4 Experimental REMPI spectrum

the repeller, lens 1, lens 2, and the SEM were +12 V, −12 V, −800 V, and −3.5 kV, respectively.

The signal intensity is recorded on a personal computer after it is amplified by a current-input preamplifier (NF, LI-76, gain: 10^4 V/A) and averaged by a boxcar integrator (NF, BX531). Since the detector has very high impedance, the signal is easily attenuated in the BNC cable from the detector to the integrator. The preamplifier also acts as an impedance converter to prevent the signal intensity from attenuating.

The wavelength step of the scanning is 0.001 nm, and the signal intensity is integrated for 128 laser pulses per each step.

4. Results and Discussions

4.1 REMPI spectra

Figure 4 represents the 2R+2 N_2-REMPI spectra of the $(v', v'')=(1, 0)$ band measured experimentally. The focal point was 5.0 mm downstream from the nozzle exit ($x/D=10$, see Fig. 3), along the center line of the jet. In this figure, the horizontal axis indicates the wavelength of the laser, and the vertical one the signal intensity normalized by that of O(10) peak, which is the maximum among the lines shown here. The dots indicate the experimental REMPI spectrum, and the broken line the simulated spectrum described in section 4.4. The source pressure and temperature were 0.60 Torr and 294 K, respectively. In this case, the number density at the focal point is 1.6×10^{13}/cm^3.

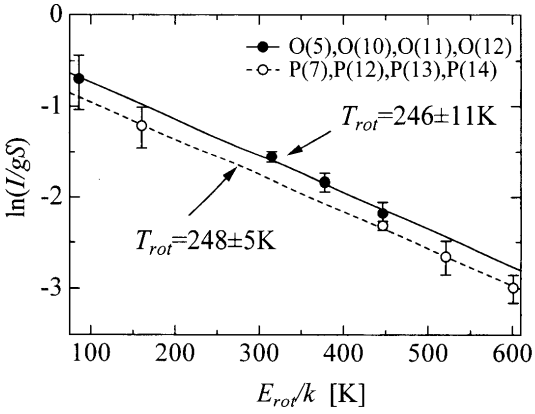

Fig. 5 Boltzmann Plot using REMPI spectra

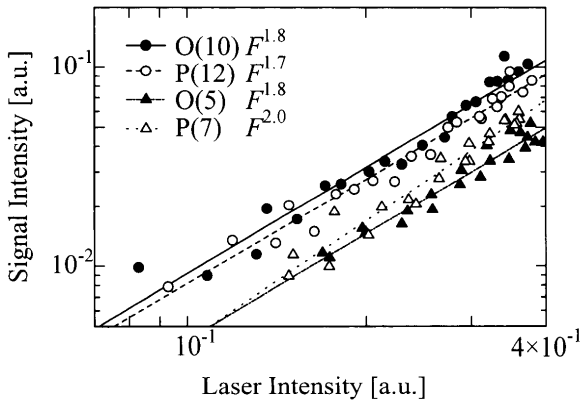

Fig. 6 Dependence of REMPI signal on laser intensity

Because the spectral lines existing from 283.4 nm to 283.57 nm are very close to one another and are usually not resolved, these lines can hardly be used for the Boltzmann plot. Therefore we did not measure the spectra in this region.

We deduced the rotational temperature at the focal point by the Boltzmann plot using the peak intensity of the spectral lines of O(5), O(10), O(11), and O(12), or those of P(7), P(12), P(13), and P(14). Figure 5 presents the Boltzmann plot using the REMPI spectra shown in Fig. 4. In this figure, the horizontal axis indicates E_{rot}/k and the vertical one $\ln(I/gS)$. The closed circles and the solid line correspond to the O branch, and the open circles and the broken line to the P branch. These straight lines are fit to the experimental data by the method of least squares, and the slope of either line corresponds to $-T_{rot}^{-1}$. As a result, the rotational temperature was deduced as 246±11 K from the O branch and 248±5 K from the P branch. From this it is confirmed experimentally that the rotational temperature deduced from the Boltzmann plot using either O or P branch agrees well with each other.

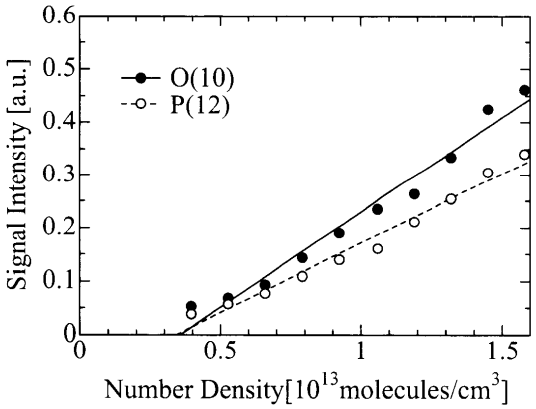

Fig. 7 Dependence of REMPI signal intensity on number density

4.2 Dependence of REMPI signal on laser intensity

Figure 6 shows the dependence of REMPI signal intensity of O(5), P(7), O(10) and P(12) on laser intensity. The horizontal axis indicates the laser intensity, which is proportional to the laser flux, and the vertical axis indicates the signal intensity. Both axes have logarithmic scales. The straight lines in the figure are decided by the least-square fitting, and the slopes of them range from 1.7 to 2.0. This dependence of the signal intensity on about F^2 (F is the laser flux) means that, as mentioned in chapter 2, most of the excited molecules at the resonant state are ionized. In this case, the REMPI spectra reflects the rotational energy distribution of the ground state.

In this paper, the effect of the fluctuation of the laser flux on the REMPI spectra is canceled by normalizing the signal by the laser flux. From the results of Fig. 6 and the investigation that will be mentioned in section 4.4, the signal should be normalized by $F^{1.7}$. Accordingly, all the experimental REMPI spectra shown in this paper are normalized by $F^{1.7}$.

At the center of the focal point, the spatial and temporal distribution of the laser flux is not uniform, but nearly Gaussian. Therefore, the reason why the dependence of the REMPI signal on the laser flux results in the power of F lower than 2 may be attributed to the partial saturation of two-photon absorption at the center of the focal point where the intensity is the highest.

4.3 Dependence of the number density on the REMPI signal

4.3.1 Limit of the number density for the temperature measurement Changing the number density at the measurement point by regulating the source pressure, we examined the number density dependence of REMPI signal at O(10) and P(12), and the limit of number density for signal detection.

Figure 7 shows the dependence of the signal inten-

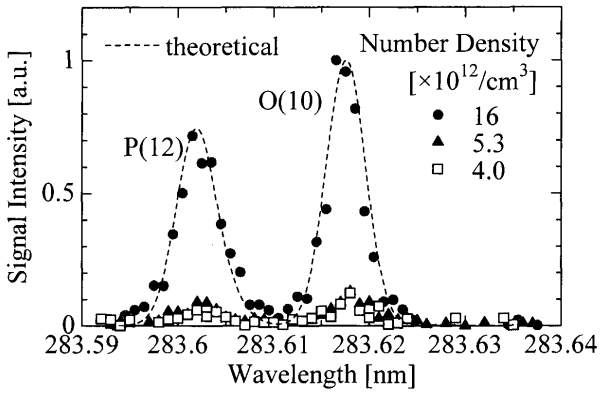

Fig. 8 Dependence of REMPI spectra on number density

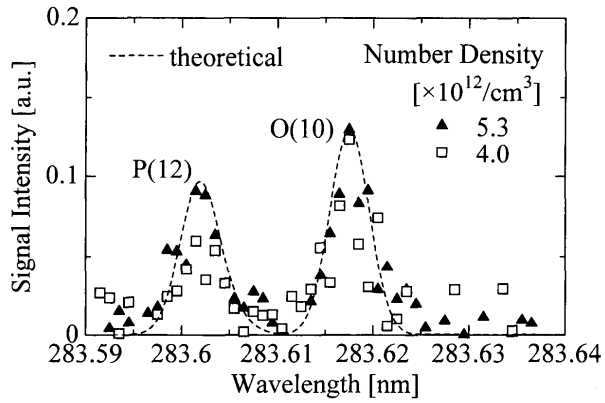

Fig. 9 REMPI spectra at low number density

sity of O(10) and P(12) on the number density at the focal point. In this figure, the horizontal axis indicates the number density at the measurement point (the focal point of the laser), and the vertical axis the signal intensity. It is obvious from this figure that the REMPI signal intensity depends almost linearly on the number density.

Figures 8 and 9 represent the REMPI spectra at the focal point for the number density of 1.6×10^{13}/cm^3, 5.3×10^{12}/cm^3, and 4.0×10^{12}/cm^3. In these figures, the horizontal axes indicate the wavelength of the laser, and the vertical ones the signal intensity normalized by that of each O(10) line. The vertical axis of Fig. 9 is enlarged so that the spectra for the relatively low number density of 5.3×10^{12}/cm^3 and 4.0×10^{12}/cm^3 can be easily compared. As can be seen, for the number density of 4.0×10^{12}/cm^3 the S/N of the spectrum is about one and the spectrum becomes blurred, indicating that the limit of the number density for the measurement of REMPI spectra using our apparatus is about 4.0×10^{12}/cm^3. Because the signal intensity of other lines used for the Boltzmann plot, such as O(5) and P(7), is comparable with that of O(10) or P(12), we can estimate the limit of the number density for the rotational temperature measurement as about 4.0×10^{12}/cm^3. This sensitivity is comparable with that of LIF method, but it could be increased by improving the apparatus as mentioned in the next subsection.

4. 3. 2 Improvements for high detection sensitivity If the laser flux or the gain of the secondary electron multiplier (SEM) is increased, the signal intensity may also be increased so that the signal can be detected even for highly rarefied gas flows. When we increased the gain of the SEM by increasing the voltage applied to the SEM, however, the level of the background noise increased more than that of the signal, and the S/N became relatively lower. Therefore, to increase the S/N, the effect of the background noise should be decreased by removing the causes of the noise.

One of the sources of the background noise seems to be the oil vapor ionized by the laser beam, which is emitted from the rotary pump used as a backing pump. To eliminate the oil vapor, a dry pump should be used as a backing pump. Instead, since these oil molecules are far heavier than nitrogen, we can separate the noise from the signal using the time-of-flight mass spectrometry (TOF-MS). To use the method, we have to set the distance from the focal point to the detector longer, though the efficiency of ion detection may be decreased.

Another source of the background noise is the ion feedback at the SEM. Since there are some neutral molecules in the SEM in our pressure condition, these molecules are ionized by electrons accelerated by the electric field in the SEM. For this problem, the background pressure at the SEM should be kept sufficiently low. To keep the background pressure low, it may be effective to separate the detection chamber from the main chamber, pumping differentially to let the background pressure of the former be lower than that of the latter.

4. 4 Boltzmann plot using multiple branches

For the Boltzmann plot using one branch, which is described in the previous paper[6] and section 4.1, the uncertainty of the slope is relatively large, leading to large uncertainty of the deduced temperature. This is because the number of the spectral lines is limited and the plot is easily affected by the measurement error of the signal intensity. However, it is difficult to increase the number of the spectral lines used for the plot, because some lines are overlapped with each other and others are too weak to be used for the plot.

As mentioned in chapter 2, if the ratios of M's in two-photon Hönl-London factors (Table 1) are determined experimentally using the spectra, it becomes possible to use multiple branches for the Boltzmann plot ; this enables to decrease the measurement error statistically for deducing the rotational temperature.

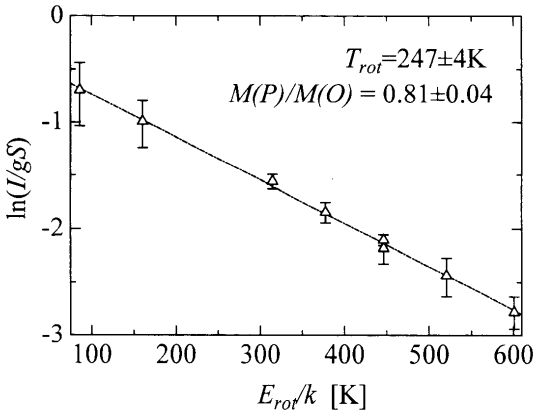

Fig. 10 Boltzmann plot using REMPI spectra (including O and P branches)

In this study, we propose the method of the Boltzmann plot using both O and P branches by determining $M(P)/M(O)$ from the experimental REMPI spectra. In Fig. 5, the interval of the two lines in the vertical direction corresponds to $|\ln[M(P)/M(O)]|$. Changing $M(P)/M(O)$ as a parameter, we determined the most suitable $M(P)/M(O)$ to minimize the square of the error between the plotted experimental data corrected by $M(P)/M(O)$ and the best fitted line calculated by the corrected data.

The laser intensity is usually not constant but it fluctuates during the scan. As mentioned in section 4.2, the intensity of the REMPI signal almost depends on the square of the laser flux. To deduce the rotational temperature accurately using the REMPI spectra, this dependence is eliminated if the signal intensity is normalized by the laser flux. Because the signal intensity depends on $F^{1.7}$-$F^{2.0}$ as shown in Fig. 6, we tried the Boltzmann plot using the REMPI spectra normalized by $F^{1.7}$, $F^{1.8}$, $F^{1.9}$, and $F^{2.0}$, to examine the dependence of the signal on the laser flux. For each case, the most suitable parameter $M(P)/M(O)$ was determined, and then we compared the square of the error between the experimental data corrected by the $M(P)/M(O)$ value and the best fitted line. As a result, the Boltzmann plot using the REMPI spectra normalized by $F^{1.7}$ and the parameter $M(P)/M(O)=0.81\pm0.04$ leads to the least square of the error. Figure 10 shows the Boltzmann plot using the parameter of $M(P)/M(O)=0.81$ and the lines of O(5), O(10), O(11), O(12), P(7), P(12), P(13), and P(14). The rotational temperature at the measurement point is deduced as 247±4 K.

To examine the validity of $F^{1.7}$ and $M(P)/M(O)=0.81$, the simulated REMPI spectrum for the deduced temperature $T_{rot}=247$ K is compared with the experimental one, as shown in Fig. 4. It is obvious that the simulated spectrum fits well with the experimental one. Moreover, this result also demonstrates the possibility of fitting method of the simulated spectrum to the experimental one as a technique for measurement of the rotational temperature.

Finally, to examine the accuracy of the rotational temperature measured from the REMPI spectra, we estimated the rotational temperature at the measurement point of the spectra ($x/D=10$) by solving the relaxation equation derived by Gallagher and Fenn[10]. To solve the equation, the rotational collision number Z_r was assumed as 4.2[11], and the Mach number distribution along the center line of a supersonic jet was estimated from the empirical formula derived by Ashkenas and Sherman[12]. Because this formula can be applied only to supersonic region, we fitted an eighth-degree polynomial to the Mach number distribution measured at University of California, Berkeley[12] to estimate the Mach number of a transonic region near the nozzle exit. As a result of this estimation, $T_{rot}=235$ K was deduced at $x/D=10$. This rotational temperature is slightly lower than that deduced from the REMPI spectra. Generally, Z_r depends strongly on the experimental conditions such as stagnation temperature and pressure[13]. The Z_r value for our experimental condition may be slightly larger than 4.2. To determine the correct Z_r value for our experimental conditions, the dependence of the rotational temperature on x/D must be analyzed by precise experimental data.

5. Conclusions

To confirm the 2R+2 N_2-REMPI method for measurements of rotational temperatures for highly rarefied gas flows, we have developed the experimental apparatus for the measurement of the REMPI signal, and the experimental REMPI spectra on the center line of a supersonic free jet have been measured. The following concluding remarks can be made:

(1) For our apparatus, the signal intensity I depends on $F^{1.7}$ (F is the laser flux). This result indicates that, in the condition of our experiment, most of the excited molecules at the resonant state are ionized. Thus the 2R+2 N_2-REMPI spectra reflects the rotational energy distribution of the ground state.

(2) The intensity of the REMPI signal depends almost linearly on the number density of nitrogen. Further, for our apparatus, the limit of the number density for the rotational temperature measurement is 4.0×10^{12} molecules/cm^3. To improve the detection sensitivity, it may be effective to decrease the density of the background molecules as well as to increase the laser flux and the gain of the detector.

(3) We have deduced the rotational temperature from the REMPI spectra measured at $x/D=10$ using the spectral lines of the O or P branch. As a result, when the source temperature and the pressure are 294 K and 0.60 Torr, respectively, the rotational temperature is deduced as 246 ± 11 K by the O branch, and 248 ±5 K by the P branch. This reveals experimentally that the rotational temperature deduced from the Boltzmann plot using either O or P branch agrees well with each other.

(4) To enable the Boltzmann plot using both O and P branches simultaneously, the ratio between $M(P)$ and $M(O)$ in the two-photon Hönl-London factors has been determined by the experimental REMPI spectra. As a result, $M(P)/M(O)$ is determined as 0.81 ± 0.04, and the rotational temperature at $x/D=10$ is deduced as 247 ± 4 K by the Boltzmann plot using the spectral lines of both O and P branches. The simulated REMPI spectrum for the deduced rotational temperature of 247 K and $M(P)/M(O)=0.81$ fits the experimental one very well, showing the effectiveness of the Boltzmann plot using multiple branches. Moreover, this result also leads to the possibility of fitting method of the simulated spectrum to the experimental one as a measurement technique for the rotational temperature.

Acknowledgements

The present work was supported by a grant-in-aid for Scientific Research (B) and "Molecular Sensors for Aero-Thermodynamic Research (MOSAIC)", the Special Coordination Funds, of Ministry of Education, Culture, Sports, Science and Technology.

References

(1) Dankert, C., Cattolica, R. and Sellers, W., Local Measurement of Temperatures and Concentrations: A Review for Hypersonic Flows, New Trends in Instrumentation for Hypersonic Research, (1994), pp. 563-581.

(2) Niimi, T., Fujimoto, T. and Shimizu, N., Method for Planar Measurement of Temperature in Compressible Flow Using Two-line Laser-Induced Iodine Fluorescence, Opt. Lett., Vol. 15, No. 16 (1990), pp. 918-920.

(3) Hara, Y., Fujimoto, T., Niimi, T., Fukuda, Y. and Oba, H., Measurement of Temperature and Number Density by CARS: Application to Plasma Jets, Rarefied Gas Dynamics: Space Science and Engineering, AIAA, Vol. 160 (1992), pp. 360-370.

(4) Carleton, K.L., Welge, K.H. and Leone, S.R., Detection of Nitrogen Rotational Distributions by Resonant 2+2 Multiphoton Ionization through the $a^1\Pi_g$ State, Chem. Phys. Lett., Vol. 115, No. 6 (1985), pp. 492-495.

(5) Lykke, K.R. and Kay, B.D., Two-photon Spectroscopy of N_2: Multiphoton Ionization, Laser-induced Fluorescence, and Direct Absorption via the $a''\Sigma_g^+$ State, J. Chem. Phys., Vol. 95, No. 4 (1991), pp. 2252-2258.

(6) Mori, H., Ishida, T., Hayashi, S., Aoki, Y. and Niimi, T., A Study on REMPI as a Measurement Technique for Highly Rarefied Gas Flows (Simulations and Its Fundamental Properties of REMPI Spectra), JSME Int. J., Vol. 43, No. 3, B (2000), pp. 400-406, (Japanese original: Trans. Jpn. Soc. Mech. Eng., Vol. 65, No. 637, B (1999), pp. 3035-3041).

(7) Bruno, A.E., Schubert, U., Neusser, H.J. and Schlag, E.W., Resonantly Enhanced 2+2 Multiphoton Ionization Spectra of N_2 via the $\tilde{a}^1\Pi_g$ State: A Line Intensity Study, Chem. Phys. Lett., Vol. 131, No. 1-2 (1986), pp. 31-36.

(8) Bray, R.G. and Hochstrasser, R.M., Two-Photon Absorption by Rotating Diatomic Molecules, Mol. Phys., Vol. 31, No. 4 (1976), pp. 1199-1211.

(9) Halpern, J.B., Zacharias, H. and Wallenstein, R., Rotational Line Strengths in Two- and Three-Photon Transitions in Diatomic Molecules, J. Mol. Spectrosc., Vol. 79 (1980), pp. 1-30.

(10) Gallagher, R.J. and Fenn, J.B., Relaxation Rates from Time of Flight Analysis of Molecular Beams, J. Chem. Phys., Vol. 60, No. 9 (1974), pp. 3487-3491.

(11) Miller, D.R. and Andres, R.P. Rotational Relaxation of Molecular Nitrogen, J. Chem. Phys., Vol. 46, No. 9 (1967), pp. 3418-3423.

(12) Ashkenas, H. and Sherman, F.S., The Structure and Utilization of Supersonic Free Jets in Low Density Wind Tunnels, Proceedings of 4th International Symposium on Rarefied Gas Dynamics, Vol. 2 (1966), pp. 84-105.

(13) Nazari, B.K., Beylich, A.E. and Dankert, C., Rotational Temperature Measurements in the New DLR-High Vacuum Test Facility STG by Means of REMPI, Proceedings of 21st International Symposium on Rarefied Gas Dynamics, Vol. 1 (1999), pp. 583-590.